炎症性腸疾患の治療におけるCXCL12/CXCR4系の意義

（分担研究者：千葉　勉）
発表者：仲瀬裕志

[背景]

・IBDの病態は1つの細胞からでは語れない。APC、好中球、CD4のT-cell等が絡み合って腸炎がおこる。この中でどこをターゲットにするかということは難しいが、白血球除去の話でもあるように白血球の遊走に関する分子を制御すれば白血球除去と同じような効果が見られるのではないか。

⇒ケモカイン

① 分子量10kD前後の主として塩基性・ヘパリン結合性サイトカインの一群である。
② ヒトでは45種類のケモカインと19種類のレセプターが同定されている。
③ ケモカインは様々な体細胞から構成的あるいは誘導性に産生される。
④ 白血球の遊走を主作用とする。
⑤ 二種類の膜結合型分子も存在。

・ケモカインのレセプターとケモカインの関係は非常にたくさんあるが、現在検討しているのは2つでCXCR4とCXCL12である。

・CXCR16は現在検討中。次年度報告したい。

・今回のターゲッティングはCD4陽性T細胞である。

＜CXCL12-CXCR4 Axis＞

・ CXCL12はSDF-1のことである。これは胎生期のB細胞の生成、骨髄での骨髄球系の増血に必須であることがわかった。SDF-1やCXCL12の欠損マウスの骨髄球系の増血は肝臓で差がないにも関わらず、骨髄では著減していた。これはSDF-1がストロマーセルから産生され増血管細胞あるいは前駆細胞の骨髄定着に必須の役割を果たしていることが始まりである。
・ この系はphysiologicalにはそうであるがpathologicalなところでも色々と役割を果たしている。たとえば、癌でも非常に重要であり、CXCR4を持っている細胞は12のあるところにたくさんトラフィックする。⇒転移等に関わっている系ではないか？ということで癌では注目されており、これに関するアンタゴニストが使用されている。IBDではどうなのか全くわかっていない。

・近年、CXCL12/CXCR4系が慢性関節リウマチをはじめとする慢性炎症性疾患の病態に関与しているとの報告がなされた。

・炎症性腸疾患の病態におけるCXCL12/CXCR4系の関与についてはいまだ不明である。

[目的]

・炎症性腸疾患の病態生理におけるCXCL12/CXCR4系の関与の検討

[結果]

・ 実際にIBDで調べてみたところ、クローン病では大きな差はないが、UCの方は差はありそうである。
・ CRPとCAIは相関しないがCXCR4とCAIは相関する。⇒UCにおいてはマーカーとして使えるかもしれない。
・ クローン病でCDAIと見たが全く相関はなかった。
・ CAP療法で効いた人はCXCR4の末血での発現は下がる。Non responder群では変化なし。

⇒潰瘍性大腸炎においての末梢血T細胞におけるCXCR4の発現はいわゆるバイオアクティブマーカーになるのではないかと考える。

[腸炎モデルマウスでの検討1]

＜方法＞

－評価方法－

DSS腸炎マウスの末梢血液中の血球細胞上のCXCR4の発現をフローサイトメトリーを用いて検討した。大腸組織内でのCXCL12の発現を蛍光免疫染色検査、およびReal-time PCR法を用いて検討した。

＜結果＞

・ 最終日sacrificeの時のデータ　CD4+、CD8+は日数が経つにつれて末梢血のCXCR4の発現は上がっていく。もともとB細胞でみつけられたのでB細胞は強い。
・ CXCL12の抗体がないため、CXCL12をノックインしたマウスを作り発現を調べた。

⇒どこに出ているか検討したところ、上皮の間に挟まっている裏打ちするような細胞に出ていることがわかった。炎症をおこすと増えるので組織で見るとすぐわかるが、PCRをしてみると当然上がってくることがわかった。

⇒おそらく炎症がおこると腸管の粘膜にCXCL12が出現し、CXCR4がたくさん出てきた細胞が集まってくるのではないかと考えた。

[腸炎モデルマウスでの検討2]

・マウス：8から12週のC57BLSマウスを用いて検討。

＜DSS腸炎の治療プロトコール＞

2.5%のDSSを5日間自由飲水させる。その後、水に切り替え、5日間飼育し、DSS投与後10日目にマウスを検討した。CXCR4の拮抗物質であるTN14003はDSS投与前日より1日2回25μg腹腔内注射した。

＜評価＞

TN14003の効果についてはマウスの体重変化、腸管長、腸管膜リンパ節の細胞数、および腸組織における炎症の程度で評価を行った。

＜結果＞

・治療群はレイトのフェーズで見るとリンパ球の浸潤が目立ち、一部ホリクルも見られる。無治療群は細胞浸潤があるが、ホリクルが結構増えてくるので、効いているという印象がある。
治療群と無治療群では有意な差が見られた。

・免疫染色をしてみると治療群ではCD4+、CD8+T細胞の浸潤が落ちている。

・DSSで投与を行うとIL10が上がり、IFN-γが下がる。

⇒mesentelicを解析してみると不思議なことにCD4+でCD25-細胞のCXCR4の発現は上がってくるが、CD4+、CD25+のCXCR4の発現はもともと高く全く変化がない。fox P3を見てみると実際に治療した群は全く変わらない。このアンタゴニスト、mesentelic lymph nodesのTregはもともとCXCR4の発現が高く、トラフィックしている状況である。このアンタゴニストを使ったとしてもおそらく局所でのTregに影響を与えないであろう。その結果、IL10の産生は少し上がり、IFN-γはカウンターで下がっていくと考えられた。

[結語]

・CXCR4 CXCL12 axis系を抑制することが腸炎の改善につながる可能性が示唆された。Tregに影響を与えることが少ないことから、CXCR4の阻害剤はIBDに対する新しい治療法の1つになればと考えている。

[質疑応答]

Q:クローン病では有意差は出ないが、なぜUCでは有意差が出たのか？

A:CXCR4の発現を促進するのはIL7である。サイミックスCD34はIL7が入ることによりCXCR4の発現をあげてしまう。今わかっているのはそこまで。他のサイトカインでCXCR4をモジュレイトすることはわかっていない。唯一IL7が鍵であると考えている。

Q:製剤(治療薬)としての見込みは？開発状況など？

A:特許をアメリカが押さえていることが判明した。これからどうしようかと考えている。

事務局連絡

［今後の予定］

平成19年度スケジュール

・平成20年2月22日（金）：分担研究者報告書類提出　締め切り

・平成20年3月7日（金）：収支決算報告書類提出　締め切り

平成20年度スケジュール（予定）

・平成20年8月1日（金）：第1回総会

IX. 研究成果の刊行物・別刷

Involvement of Smad3 phosphoisoform-mediated signaling in the development of colonic cancer in IL-10-deficient mice

DAISUKE HACHIMINE[1], KAZUSHIGE UCHIDA[1], MASANORI ASADA[2], AKIYOSHI NISHIO[2], SEIJI KAWAMATA[1], GO SEKIMOTO[1], MIKI MURATA[1], HIDEO YAMAGATA[1], KATSUNORI YOSHIDA[1], SHIGEO MORI[1], YOSHIYA TAHASHI[1], KOICHI MATSUZAKI[1] and KAZUICHI OKAZAKI[1]

[1]Third Department of Internal Medicine, Kansai Medical University, Moriguchi City, Osaka;
[2]Department of Gastroenterology, Graduate School of Medicine, Kyoto University, Kyoto, Japan

Abstract. Chronic inflammation predisposes to cancer. Transforming growth factor (TGF)-ß, a multifunctional protein, suppresses the growth of normal colonic epithelial cells, whereas it stimulates the proliferation of cancer cells. Interleukin (IL)-10-deficient mice, which develop colitis and colorectal cancer, show an increased level of plasma TGF-ß. Although TGF-ß may be a key molecule in the development of colon cancer arising from chronic colitis in IL-10-deficient mice, the role of TGF-ß still remains unclear. TGF-ß activates not only TGF-ß type I receptor (TßRI) but also c-Jun N-terminal kinase (JNK), which converts the mediator Smad3 into two distinctive phosphoisoforms: C-terminally phosphorylated Smad3 (pSmad3C) and linker-phosphorylated Smad3 (pSmad3L). We studied C57BL/6-IL-10-deficient mice (n=18) at 4 to 32 weeks of age. We investigated histology, and pSmad2/3L, pSmad2/3C, and p53 by immunohistochemistry. pSmad3L staining was detected in the cancer cells in all 10 mice with colonic cancer and in the epithelial cells in 7 of 12 mice with colonic dysplasia, but not in the normal or colitic mice. pSmad3c was detected without any significant difference between stages. p53 was weakly stained in a few cancer cells in 5 out of 10 mice. Smad3L signaling plays an important role in the carcinogenesis of chronic colitis in IL-10-deficient mice.

Introduction

In 1925, Crohn and Rosenberg documented a case of rectal carcinoma complicating ulcerative colitis (UC) and postulated that the lesion developed as a late manifestation of the disease (1), and many subsequent epidemiological studies have confirmed this increased risk (as high as 34%) after 25 years of disease (2). In contrast to sporadic colorectal cancers, which develop through the 'adenoma-carcinoma sequence', inflammatory bowel disease (IBD)-associated carcinomas develops through the 'dysplasia sequence'. Although cancers from UC as well as sporadic colorectal carcinoma are hypothesized to arise from a multistep process, the precise mechanism is still unknown.

Interleukin (IL)-10-deficient mice under specific-pathogen free conditions spontaneously develop chronic enterocolitis, a condition phenotypically similar to chronic IBD in humans (3). An increase in the incidence rate of colorectal carcinoma has been observed in conjunction with elevated plasma transforming growth factor (TGF)-ß1 levels at 10 to 31 weeks of age (4), which suggests that TGF-ß may be a key molecule in the development of colon cancer arising from chronic colitis in IL-10-deficient mice. Therefore, this murine IBD model may provide excellent insights into the pathogenetic mechanism of chronic colitis-associated carcinoma.

TGF-ß is a multifunctional protein that regulates a complex array of cellular processes, including proliferation, differentiation, motility, and death in a cell-specific manner (5). TGF-ß can inhibit colonic epithelial cell growth, acting as a tumor suppressor (6) and also plays a major role in the negative regulation of immune cell functions, particularly in the gut (7). Loss of TGF-ß (8) or unresponsiveness to TGF-ß1 (9) in the colonic epithelium has been associated with the development or progression of inflammation in the colon. However, increased TGF-ß activity may be involved in tumor development rather than tumor suppression in IL-10-deficient mice (5). The role of TGF-ß in tumor development thus seems to be dual, and dependent on the stage of the tumor. These multiple functions are thought to result from different intracellular signaling pathways. Recent evidence suggests that TGF-ß is also a key regulator of epithelial-to-mesenchymal transition (EMT) in cell phenotypes (10). EMT not only underlies epithelial degeneration and fibrogenesis in chronic degenerative disorders, but also endows dedifferentiated malignant epithelial cells with mesenchymal, migratory, and proteolytic properties that are required for local tumor invasiveness (11). Inhibition of the pro-inflammatory cytokine IL-1ß at initiation of EMT has been

Correspondence to: Dr Kazuichi Okazaki, Third Department of Internal Medicine, Kansai Medical University, 10-15 Fumizono-cho, Moriguchi City, Osaka, 570-8506, Japan
E-mail: okazaki@hirakata.kmu.ac.jp

Key words: Smad3, colonic cancer, interleukin-10

found to attenuate fibrogenesis (12), suggesting a causative link between chronic inflammation and EMT. The main downstream signaling pathway for TGF-ß involves the Smad proteins (13). Although several studies of EMT have suggested that the process involves Smad-independent pathways (14), recent studies using Smad3 knockout mice have indicated that signaling through the Smad3-dependent pathway is required for injury-dependent multistage transition of an epithelial cell to a mesenchymal phenotype (15). Therefore, we focused on Smad3 signaling (16,17), and on the different roles of Smad3 phosphoisoform-mediated signaling in epithelial cells and mesenchymal cells, reported recently (18). Thus, TGF-ß activates not only TGF-ß type I receptor (TßRI) but also c-Jun N-terminal kinase (JNK), converting Smad3 into two distinct phosphoisoforms: C-terminally phosphorylated Smad3 (pSmad3C) and linker-phosphorylated Smad3 (pSmad3L). The TßRI/pSmad3C pathway inhibits growth of epithelial cells, while JNK/pSmad3L-mediated signaling promotes ECM deposition by activated mesenchymal cells such as hepatic stellate cells (HSCs) (5). However, it is unclear how Smad3 signaling is involved in the development of colon cancer during long-standing chronic colitis.

In the present study, according to these phosphorylation-defined activities, we studied whether Smad3 phosphoisoforms govern progression from chronic colitis to colonic cancer in an IL-10-deficient mouse model.

Materials and methods

Animals. C57BL/6-IL-10-deficient mice (aged 4-32 weeks) were purchased from The Jackson Laboratory (Bar Harbor, ME). The animals were housed under specific-pathogen free (SPF) conditions and fed autoclaved food and sterile water in the animal facility of the Graduate School of Medicine, Kyoto University. Of these, the IL-10-deficient mice were transferred from SPF to conventional housing conditions at six weeks of age as they spontaneously develop colitis under conventional housing conditions by eight weeks of age. All animal experiments were performed in accordance with our institutional guidelines.

Histology. The entire large intestines were examined in 18 IL-10-deficient mice between 4 and 32 weeks of age. The large intestines were fixed in 4.5% buffered formaldehyde before embedding in paraffin blocks. For histological analysis, 5-μm sections were cut and stained with hematoxylin and eosin (H&E). The principal histologic distinction was between dysplasia and colorectal carcinoma according to Japanese criteria. Histologic slides involving diagnoses of normal, dysplasia and adenocarcinoma were reviewed independently by two pathologists specialising in gastrointestinal neoplasia.

Domain-specific Abs against the phosphorylated Smad3. Polyclonal anti-phospho-Smad3 antibodies [anti-pSmad3L ($Ser^{207/212}$) and anti-pSmad3C ($Ser^{423/425}$)] were raised against the phosphorylated linker regions and COOH-terminal regions of Smad3 by immunization of rabbits with synthetic peptides. The relevant antisera were affinity purified with the phosphorylated peptides as described previously (16).

Table 1. Serial analysis of intestines in IL-10-deficient mice.

Age (weeks)	n	Colitis	Dysplasia	Cancer
4	3	0	0	0
7	1	1	0	0
8	2	2	2	0
12	2	2	2	1
16	2	2	2	2
24	2	2	2	2
28	4	4	4	4
32	2	2	2	2

Immunohistochemistry. Immunohistochemical staining was performed on formalin-fixed, paraffin-embedded tissue sections. The sections were deparaffinized in xylene, and rehydrated in graded alcohols. Antigen retrieval was done by microwave irradiation in 0.01 M sodium citrate buffer (pH 6.0) for 15 min. After cooling, the endogenous peroxidase activity was blocked by incubation in 3% H_2O_2 in methanol for 10 min. After rinsing with TBS containing 0.1% Tween-20 (TBST), non-specific antigens were blocked by preincubation with 1% bovine serum albumin (Nakarai, Kyoto, Japan). The sections were incubated overnight with the following primary antibodies: anti-mouse p53 (1.0 μg/ml, Abcam, Cambridge, UK), anti-pSmad3L (1 μg/ml) and anti-pSmad3C (1 μg/ml). After rinsing with TBST, the sections were incubated with peroxidase-labeled polymer conjugated to goat anti-rabbit immunoglobulin for 1 h at room temperature. The peroxidase activity was visualized with 3,3'-diaminobenzidine (Vector Laboratories, Burlingame, CA) counterstained with Mayer's hematoxylin (Merck, Darmstadt, Germany), and mounted under coverslips. The evaluation of immunoreactivity was performed by microscopy (Olympus BX 50, Tokyo, Japan). Immunohistochemistry was scored by pathologists in double-blind fashion according to staining proportions as follows: 0, no staining seen; 1, staining seen in 5-30% of cells; 2, staining seen in >30% of cells.

Statistical analysis. Statistical evaluation was done using the nonparametrical Mann-Whitney U ranking test. Values were based on two-tailed statistical analysis.

Results

Development of colorectal dysplasia and carcinomas in IL-10-deficient mice. We confirmed a previous report that IL-10-deficient mice develop colitis after 7 weeks. We found that mice developed dysplasia or cancer after 8 to 12 weeks, respectively (Table I; Fig. 1). We observed no metastasis in the mesenteric lymph nodes or liver in any mice. We also observed that the small intestine was not affected.

Smad3 phosphorylation of COOH-terminals and linker regions. Immunohistochemical analysisis was performed on mice from each stage to detect Smad3 phosporylation. pSmad3C was detected without significant difference between

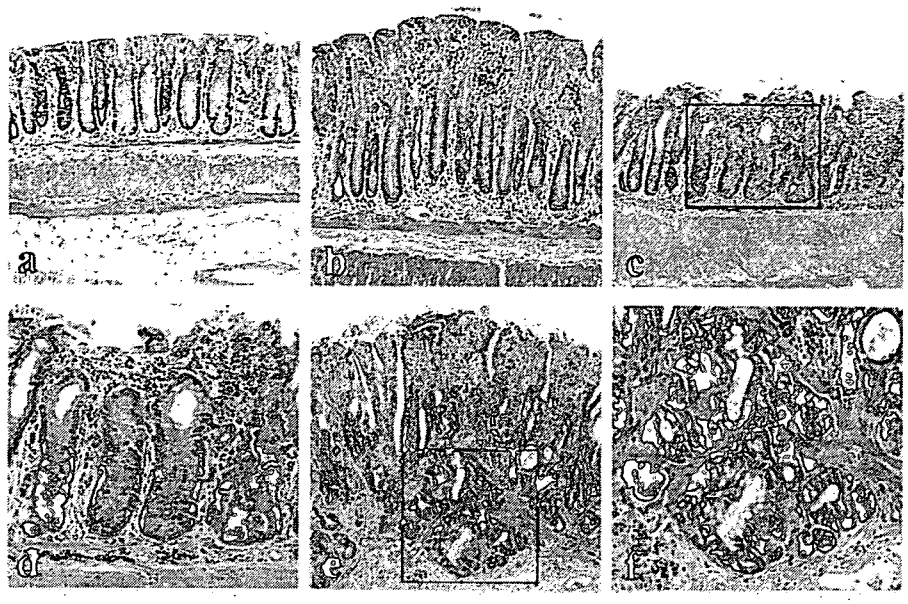

Figure 1. Histopathological findings of the colorectum in IL-10-deficient mice using hematoxylin and eosin staining (H&E). Normal colonic mucosa (a, x40). IL-10-deficient mice developed colitis (b, x40) after 7 weeks. Dysplasia (c, x40; d, x200) and cancer (e, x40; f, x200) were found after 8-12 weeks.

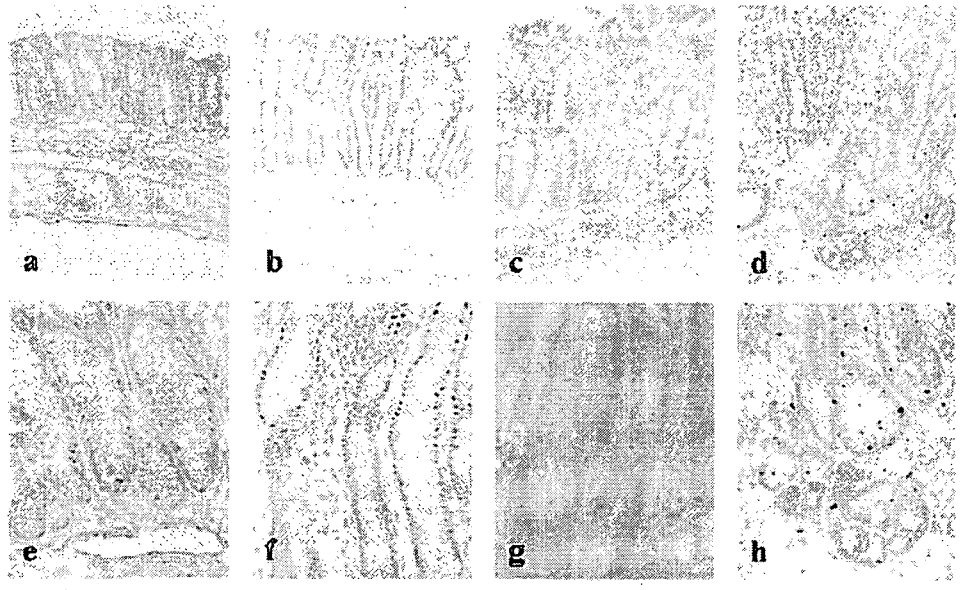

Figure 2. Immunohistochemical findings of the colorectum in IL-10-deficient mice using anti-pSamd3C antibody. pSmad3C was detected without significant difference between stages. Normal mucosa (a, x40; e, x200); colitis (b, x40; f, x200); dysplasia (c, x40; g, x200); cancer (d, x40; h, x200).

stages (Figs. 2 and 5). On the other hand, pSmad3L detection levels gradually increased from dysplasia to adenocarcinoma (Figs. 3 and 5). pSmad3L was expressed in dysplasia and cancer cells, but not in inflamed mucosa cells, even in the mice with cancer.

p53 expression in colorectal cancers. To determine p53 expression, all mice were subjected to immunohistochemical analysis using rabbit anti-mouse p53 polyclonal antibody. p53 was detected only in the mice with colonic cancer (Figs. 4 and 5). Dysplasia of the colorectal epithelium was not stained with anti-p53 antibody (Figs. 4 and 5). In 5 out of the 10 mice with cancer, the cancer cells were stained, however very few cells were p53 positive and even so stained weakly (Figs. 4 and 5).

Discussion

Colon cancer in patients with ulcerative colitis is thought to be associated with long-standing tissue injury and chronic inflammation (19). The relationship between chronic inflammation and cancer dates back to Virchow, who, in

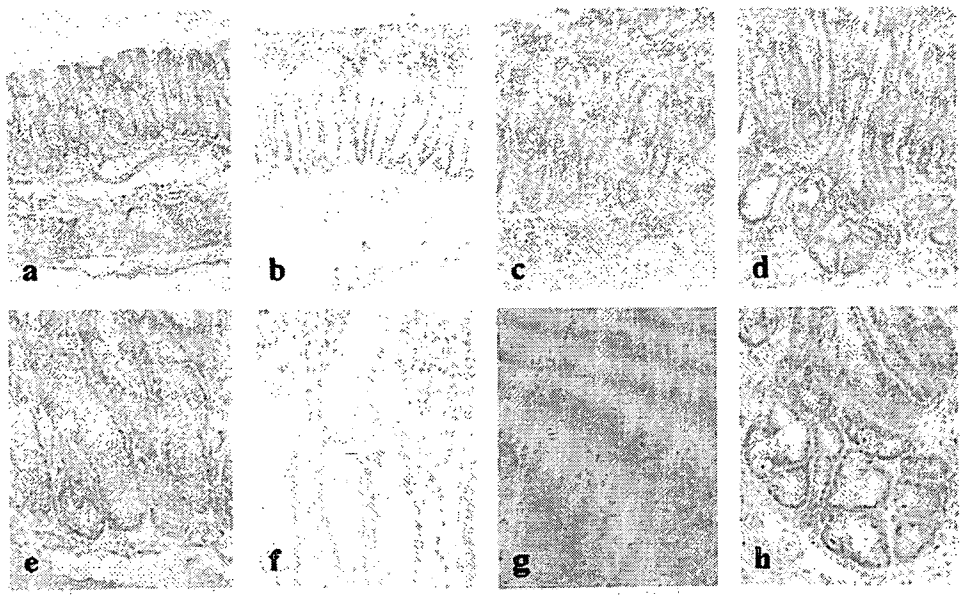

Figure 3. Immunohistochemical findings of the colorectum in IL-10-deficient mice using anti-pSamd3L antibody. pSmad3L detection levels gradually increased from dysplasia to adenocarcinoma. Normal mucosa (a, x40; e, x200); colitis (b, x40; f, x200); dysplasia (c, x40; g, x200); cancer (d, x40; h, x200).

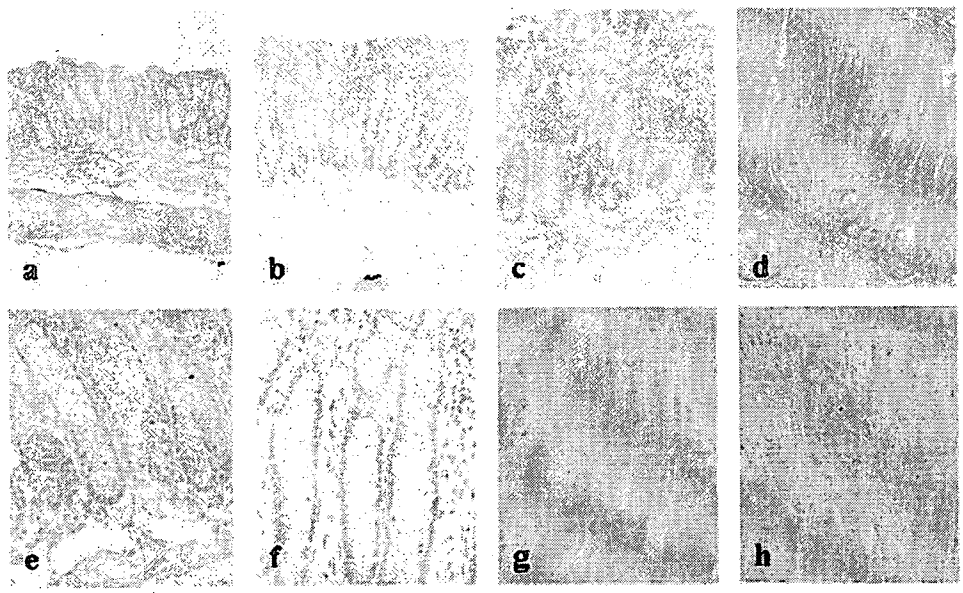

Figure 4. Immunohistochemical findings of the colorectum in IL-10 deficient mice using anti-p53 antibody. In 5 out of 10 mice with cancer, a few cancer cells were stained weakly. Normal (a, x40; e, x200); colitis (b, x40; f, x200); dysplasia (c, x40; g, x200); cancer (d, x40; h, x200).

1863, hypothesized that the origin of cancer was at sites of chronic inflammation (20). Although the relation between chronic inflammation and cancer has been well established in general, the molecular mechanisms involved in the process remain unclear. Certainly, chronic inflammation leads to increased oxidative stress. Leukocytes and other phagocytic cells generate reactive oxygen and nitrogen species, which, in turn, can damage proliferating epithelial cells. Also, chronic inflammation appears to promote the apoptosis of normal epithelial cells which can lead to a compensatory proliferative response by the remaining tissue.

Our present study confirmed that IL-10-deficient mice, spontaneously develop colonic dysplasia and cancer at a high rate following chronic colitis (4). In IL-10-deficient mice, it has been shown that serum levels of TGF-ß1 significantly increase in mice with dysplasia and cancer, compared to those without tumors (4). This led us to a hypothesize that genetic alterations in other members of the TGF-ß receptor signal transduction pathway are involved in the development of colon cancer in long-standing colitis. TGF-ß, which can potently inhibit epithelial cell growth to act as a tumor suppressor (10), is also a key regulator of epithelial-to-

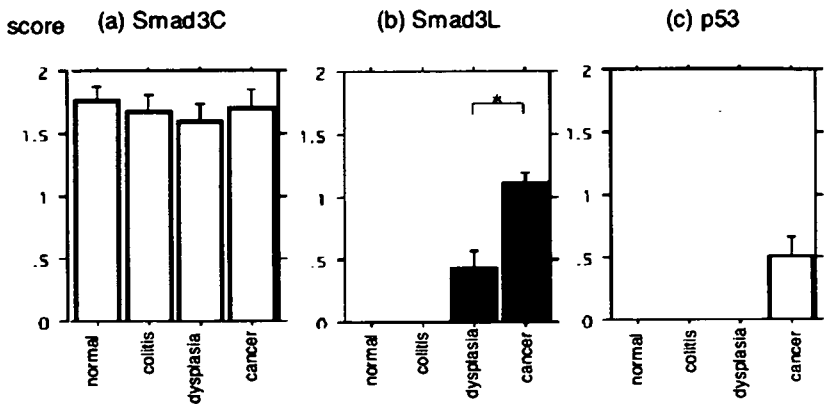

Figure 5. Immunohistochemical scores of Smad3C, 3L and p53. Immunohistochemistry was scored by pathologists in double-blind fashion according to staining proportions as follows: 0, no staining seen; 1, staining seen in 5 to 30% of cells; 2, staining seen in >30% of cells. pSmad3L detection levels increased significantly from colitis to dysplasia (0.417±0.513) to adenocarcinoma (1.100±0.316) ($p<0.05$). In normal and inflamed mucosa, even in cancerous mice, pSmad3L was not detected. Cancer cells were also stained with p53, however very few cells were positive and even so stained weakly (0.500±0.527). pSmad3C was detected without any significant difference between stages. Scores of pSmad2C staining in normal mucosa, colitis, dysplasia, and cancer were: 1.750±0.452, 1.667±0.492, 1.583±0.515, and 1.700±0.483, respectively.

mesenchymal transition (EMT) in cell phenotypes. EMT may be related to the loss of tumor responsiveness on the growth inhibitory effect of TGF-ß and at the same time to the TGF-ß-induced angiogenesis, and local and systemic immunosuppression. During carcinogenesis, tumors show EMT, thereby becoming insensitive to TGF-ß-mediated growth inhibition while showing increased tumor invasion and metastasis (10,21).

TGF-ß signaling is initiated when this ligand induces the formation of a heteromeric complex composed of TGF-ß receptor type I (TßRI) and type II (TßRII). This allows TßRII to phosphorylate TßRI, which then transmits the signal through phosphorylation of receptor-regulated Smads (R-Smads) such as Smad2 and Smad3 (22). R-Smads are directly phosphorylated at COOH-terminal SXS regions by TßRI and then undergo formation of heteromeric complexes with Smad4 (23). Activated Smad complexes are then translocated into the nucleus, where they regulate the expression of target genes both by direct DNA binding and through interaction with other transcription factors, co-activators, and co-repressors (24). Smads contain two highly conserved domains, the Mad homology 1 (MH1) and 2 (MH2) domains, which are connected by interposed linker regions (25). Although the MH1 domains can interact with DNA, the MH2 domains are endowed with transcriptional activation properties (23). In human colorectal cancer, somatic mutation of the Smad4 (18q21) or Smad2 gene (18q21) has been detected in the MH2 domain, but mutations of Smad3 (15q21), Smad6 (15q21), and Smad7 (18q21) genes have not been detected so far (26). On the other hand, Smad3-deficient mice develop colorectal carcinoma (27). Although several studies of EMT have suggested that the process involves Smad-independent pathways (23), there is evidence from Smad3-deficient mice that signaling through the Smad3-dependent pathway is required for injury-dependent multistage transition of an epithelial cell to a mesenchymal phenotype (15). As a consequence, we have focused on Smad3 signaling (16,17) and successfully developed polyclonal antibodies, which specifically recognize the phosphorylated linker regions and phosphorylated COOH-terminal SXS regions of Smad3 (17). Using these antibodies, we recently reported that Smad3 phosphorylated at linker regions or COOH-terminal regions existed as separate molecules with different functions and transmitted distinct signals (16-18). We also previously reported that as neoplasia progresses from normal colorectal epithelium through adenoma to invasive adenocarcinoma with distant metastasis, nuclear pSmad3L gradually increases while pSmad3C decreases (28). The TßRI/Smad pathway is widely represented in most cell types and tissues studied to date, and additional pathways are activated following cell stimulation by TGF-ß in specific contexts. The most prominent pathways are mediated by the mitogen activated protein kinase (MAPK) family, which consists of the extracellular signal-regulated protein kinase pathways c-Jun NH2-terminal kinase (JNK) and p38 pathways (29). TGF-ß induces activation of MAPK pathways through the upstream mediators Ras, RhoA, PP2A, and TGF-ß-activated kinase I (17). Thus, TGF-ß activates not only TßRI but also JNK, which converts Smad3 into two distinctive phosphoisoforms: pSmad3C and pSmad3L (5). Therefore, during sporadic human colorectal carcinogenesis, the shift from TßRI/pSmad3C-mediated to JNK/pSmad3L-mediated signaling is a major mechanism orchestrating a complex transition of TGF-ß signaling (5).

In the present animal study, we observed a significant increase in pSmad3L as neoplasia progressed from normal colorectal epithelium through dysplasia. Our study showed that, unlike human sporadic colon cancer, there were no changes in the phosphorylation of pSmad3C in the murine model. Moreover, no mice showed deep invasion and metastasis of cancer, which suggested that the malignant potential might be low in IL-10-deficient colitis.

The p53 mutation is known as the most common cancer-related genetic change (30). The overexpression of p53 occurs frequently in ulcerative colitis-associated colorectal carcinoma regardless of stage and pathological characteristics (31). In our results, p53 could only be detected in

some cancerous cells, and positive staining was weak. These findings, together with previous reports suggest that *p53* mutations are unlikely to be involved in the malignant transformation of epithelial cells in mice (4). Also, inactivation of *p53* may occur in the late stages of colorectal cancers developing in IL-10-deficient mice, thus being present in only a small number of tumor cells and barely detectable by the methods used in our study.

In conclusion, the phosphorylation of Smad3L may play an important role in the carcinogenesis of colorectal cancer associated with chronic colitis in IL-10-deficient mice. Further studies in human ulcerative colitis are necessary for the clarification of colitic cancer.

Acknowledgements

This study was partly supported by Grants-in-Aid for scientific program (C) from the Ministry of Science and Culture of Japan (18590755), and by Grants-in-Aid from the Health, Labor and Welfare Ministry of Japan.

References

1. Crohn BB and Rosenberg H: The sigmoidscopic picture of chronic ulcerative colitis (non-specific). Am J Med Sci 170: 220-228, 1925.
2. Kewenter J, Ahlman H and Hulten L: Cancer risk in extensive ulcerative colitis. Ann Surg 188: 824-828, 1978.
3. Reninick DM, Fort MM and Davidson NJ: Studies with IL-10-/- mice; an overview. J Leukoc Biol 61: 389-396, 1997.
4. Strulan S, Oberhuber G, Beinhauer BG, Tichy B, Kappel S, Wang J and Rogy MA: Interleukin-10-deficient mice and inflammatory bowel disease associated cancer development. Carcinogenesis 22: 665-671, 2001.
5. Matsuzaki K and Okazaki K: Transforming growth factor-beta during carcinogenesis: the shift from epithelial to mesenchymal signaling. J Gastroenterol 41: 295-303, 2006.
6. Moses HL, Yang EY and Pietenpol JA: TGF-beta stimulation and inhibition of cell proliferation: new mechanistic insights. Cell 63: 245-247, 1990.
7. MacDonald TT: Effector and regulatory lymphoid cells and cytokines in mucosal sites. Curr Top Microbiol Immunol 236: 113-135, 1999.
8. Maloy KJ and Powrie F: Regulatory T cells in the control of immune pathology. Nat Immunol 2: 816-822, 2001.
9. Eppert K, Scherer WS, Ozcelik H, *et al*: MADR maps to 18q21 and encodes a TGF-ß-regulated MAD-related protein that is functionally mutated in colorectal carcinoma. Cell 86: 543-552, 1996.
10. Zavadil J and Bottinger EP: TGF-ß and epithelial-to-mesenchymal transitions. Oncogene 24: 5764-5774, 2005.
11. De Caestecker MP, Piek E and Roberts AB: Role of transforming growth factor-ß signaling in cancer. J Natl Cancer Inst 92: 1388-1402, 2000.
12. Kolb M, Margetts PJ, Anthony DC, *et al*: Transient expression of IL-1beta induces acute lung injury and chronic repair leading to pulmonary fibrosis. J Clin Invest 107: 1529-1536, 2001.
13. Heldin CH, Miyazono K and ten Dijke P: TGF-ß signaling from cell membrane to nucleus through SMAD proteins. Nature 390: 465-471, 1997.
14. Derynck R and Zhang YE: Smad-dependent and Smad-independent pathways in TGF-ß family signaling. Nature 425: 577-584, 2003.
15. Saika S, Kono-Saika S, Ohnishi Y, *et al*: Smad3 signaling is required for epithelial-mesenchymal transition of lens epithelium after injury. Am J Pathol 164: 651-663, 2004.
16. Furukawa F, Matsuzaki K, Mori S, *et al*: p38 MAPK mediates fibrogenic signal through Smad3 phosphorylation in rat myofibroblasts. Hepatology 38: 879-889, 2003.
17. Mori S, Matsuzaki K, Yoshida K, *et al*: TGF-ß and HGF transmit the signals through JNK-dependent Smad2/3 phosphorylation at the linker regions. Oncogene 23: 7416-7429, 2004.
18. Yoshida K, Matsuzaki K, Mori S, *et al*: Transforming growth factor-ß and platelet-derived growth factor signal via c-Jun N-terminal kinase-dependent Smad2/3 phosphorylation in rat hepatic stellate cells after acute liver injury. Am J Pathol 166: 1029-1039, 2005.
19. Ekbom A, Helmick C, Zack M and Adami HO: Ulcerative colitis and colorectal cancer. A population-based study. N Engl J Med 323: 1228-1233, 1990.
20. Balkwill F and Mantovani A: Inflammation and cancer: back to Virchow? Lancet 357: 539-45, 2001.
21. Oft M, Peli J, Rudaz C, Schwarts H, Beug H and Reichmann E: TGF-beta1 and Ha-Ras collaborate in modulating the phenotypic plasticity and invasiveness of epithelial tumor cells. Genes Dev 10: 2462-2477, 1996.
22. Shi Y and Massague J: Mechanisms of TGF-beta signaling from cell membrane to nucleus. Cell 113: 685-700, 2003.
23. Derynck R and Zhang YE: Smad-dependent and Smad-independent pathways in TGF-beta family signaling. Nature 425: 577-584, 2003.
24. Kretschmar M, Doody J, Timokhina I and Massague J: A mechanism of repression of TGFbeta/Smad signaling by oncogenic Ras. Genes Dev 13: 804-816, 1999.
25. Robinson MJ and Cobb MH: Mitogen-activated protein kinase pathways. Curr Opin Cell Biol 9: 180-186, 1997.
26. Miyaki M and Kuroki T: Role of Smad4 (DPC4) inactivation in human cancer. Biochem Biophys Res Commun 306: 799-804, 2003.
27. Zhu Y, Richardson JA and Parada LF: Smad3 mutant mice develop metastatic colorectal cancer. Cell 94: 703-714, 1998.
28. Yamagata H, Matsuzaki K, Mori S, *et al*: Acceleration of Smad2 and Smad3 phosphorylation via c-Jun NH2-terminal kinase during human colorectal carcinogenesis. Cancer Res 65: 157-165, 2005.
29. Mulder KM: Role of Ras and Mapks in TGFbeta signaling. Cytokine Growth Factor Rev 11: 23-35, 2000.
30. Vogelstein B: Cancer. A deadly inheritance. Nature 348: 681-682, 1990.
31. Harpaz N, Peck AL, Yin J, *et al*: p53 protein expression in ulcerative colitis-associated colorectal dysplasia and carcinoma. Hum Pathol 25: 1069-1074, 1994.

Subcutaneous Adipose Tissue-Derived Stem Cells Facilitate Colonic Mucosal Recovery from 2,4,6-Trinitrobenzene Sulfonic Acid (TNBS)-Induced Colitis in Rats

Yugo Ando,[*†] Muneo Inaba,*[*‡§] Yutaku Sakaguchi,*[*†] Masanobu Tsuda,*[*] Guo Ke Quan,*[*] Mariko Omae,*[*] Kazuichi Okazaki,[†‡§] and Susumu Ikehara*[*†§]*

Background: Adipose tissue-derived stem cells (ADSCs) can be easily obtained from subcutaneous adipose tissue, and ADSCs can be demonstrated to display multilineage developmental plasticity. In this study, using TNBS-induced colitis rats, we show the feasibility of repairing injured intestinal mucosa with adipose tissue-derived stem cells.

Methods: The subcutaneous adipose tissue of F344 rats was obtained and digested by collagenase. The digested tissue was cultured in DMEM containing 10% FBS for 1 month. ADSCs were confirmed to differentiate under appropriate conditions into various lineages of cells, including bone, neural cells, adipocytes, and epithelial cells. HGF, VEGF, TGF-β, and adiponectin in the culture supernatants of ADSCs were determined by ELISA. ADSCs (10^7 cells) were injected into the submucosa of the colon to examine their capacity to repair intestinal mucosa injured by TNBS.

Results: In the experimental colitis model, the injection of ADSCs facilitated colonic mucosal repair and reduced the infiltration of inflammatory cells. High levels of HGF, VEGF, and adiponectin were detected in the culture supernatants of ADSCs. Moreover, injected ADSCs distributed to several layers of the colon, and some of them differentiated into mesodermal lineage cells.

Conclusions: ADSCs can accelerate the regeneration of injured regions in experimental colitis. HGF, VEGF, and adiponectin might be responsible for the regeneration of injured regions in the colon.

(Inflamm Bowel Dis 2008;14:000–000)

Key Words: HGF, VEGF, adiponectin, subcutaneous adipose tissue, Crohn's disease

Crohn's disease is characterized by chronic relapsing inflammation of the gastrointestinal tract. Evidence suggesting that various immune, genetic, and environmental factors influence both the initiation and progression of colitis has been accumulated. However, the precise mechanism or mechanisms underlying the development of this disease have yet to be clarified.

In recent years, several groups have reported the ubiquitous distribution of adult stem cells in various tissues and organs, including bone marrow, muscle, brain, skin, and, more recently, even in subcutaneous fat.[1] Among these adult stem cells, those in the subcutaneous fat, termed adipose tissue-derived stem cells (ADSCs), can be easily obtained with a relatively lower burden on donors; they can be easily harvested from subcutaneous adipose tissue by lipoaspiration. These ADSCs have been demonstrated to display multilineage developmental plasticity.[2] Furthermore, ADSCs have been reported to have less heterogeneity in their immunophenotype and multilineage differentiation ability[3,4] than do bone marrow-derived mesenchymal stem cells. Because of these advantages, clinical use of ADSCs for not only fat, bone, and myocardium reproduction but also spinal cord regeneration, vascularization, and the treatment of intractable ulcers has been carried out, and the development of further clinical applications is expected. Garcia-Olmo et al[5] reported in a phase I clinical trial of Crohn's disease that after an operation to close fistula, cell therapy using autologous ADSCs can facilitate fistula repair. However, ADSCs may have, in general, a potential to treat Crohn's disease and inflammatory bowel disease (IBD) in addition to the treatment for fistula

Received for publication August 10, 2007; accepted December 4, 2007.

From the *First Department of Pathology, Kansai Medical University, Osaka, Japan; †Third Department of Internal Medicine, Kansai Medical University, Osaka, Japan; ‡Regeneration Research Center for Intractable Diseases, Kansai Medical University, Osaka, Japan; and §Center for Cancer Therapy, Kansai Medical University, Osaka, Japan.

Supported by a grant from Haiteku Research Center of the Ministry of Education; a grant from the Millennium program of the Ministry of Education, Culture, Sports, Science and Technology; a grant from the Science Frontier program of the Ministry of Education, Culture, Sports, Science and Technology; a grant from the 21st Century Center of Excellence (COE) program of the Ministry of Education, Culture, Sports, Science and Technology; a grant from the Department of Transplantation for Regeneration Therapy (sponsored by Otsuka Pharmaceutical Company, Ltd.); a grant from Molecular Medical Science Institute, Otsuka Pharmaceutical Co., Ltd.; a grant from Japan Immunoresearch Laboratories Co., Ltd. (JIMRO); and by Grant-in-Aid for inflammatory bowel disease of the Ministry of Health, Labor and Welfare.

Reprints: Susumu Ikehara, Kansai Medical University, Pathology, Osaka, Japan (e-mail: ikehara@takii.kmu.ac.jp)

DOI 10.1002/ibd.20382

Published onlinein Wiley InterScience (www.interscience.wiley.com).

observed in a subpopulation of patients with Crohn's disease. Therefore, the potential ability of ADSCs to improve mucosal healing of inflammatory lesions and the biological mechanism underlying the repair function of ADSCs should be examined. In the present study, using Crohn's disease models in rats in which the colonic mucosa is injured by TNBS, we attempted to treat the mucosal injury by a submucosal injection of ADSCs to facilitate mucosal recovery; we expected this to be a simple and safe procedure. It is noted that ADSCs injected intravenously might be trapped by the reticuloendothelial system in the liver or lung[6]; therefore, they could not be recruited to the intestinal mucosa. Thus, in this study, ADSCs were directly injected into the submucosa, and ADSCs actually facilitated the regeneration of the injured region (by TNBS injection). Furthermore, we also examined the potency of ADSCs to differentiate into various lineage cells and their production of growth factors such as HGF, VEGF, TGF-β, and adiponectin that may accelerate mucosal regeneration.

MATERIALS AND METHODS

Animals

F344/DuCrlCrlj rats were purchased from Charles River Laboratories Japan, Inc. (Yokohama, Japan), and maintained for 1 to 2 weeks in our animal facilities before the start of TNBS treatment. Rats were maintained on a 12-hour light/12-hour dark cycle under pathogen-free conditions and had a standard diet and water until reaching the desired age (13 weeks).

Isolation and Culture of Rat Subcutaneous Adipose Tissue–Derived Stem Cells (ADSCs)

The subcutaneous adipose tissue of F344 rats was obtained by abdominal incision. The raw subcutaneous adipose tissue was washed extensively with sterile phosphate-buffered saline (PBS; Gibco, Invitrogen Corporation, Carlsbad, Calif.) to remove blood cells. The extracellular matrix was digested with a solution of type II collagenase (0.075%; Gibco, Invitrogen Corporation, Carlsbad, Calif.) in balanced salt solution (5 mg/mL; Gibco, Invitrogen Corporation, Carlsbad, Calif.) for 60 minutes at 37°C to release the cellular fraction.[5] Next, the collagenase was inactivated by the addition of an equal volume of RPMI (Sigma-Aldrich, St. Louis, Mo.) containing 10% fetal bovine serum (FBS; Invitrogen Corporation, Carlsbad, Calif.). The suspension of cells was centrifuged at 250*g* for 10 minutes. Cells were resuspended in DMEM (Sigma-Aldrich, St. Louis, Mo.) plus 10% FBS. The mixture was centrifuged at 250*g*, and the cells were resuspended in DMEM plus 10% FBS and a 1% ampicillin/streptomycin mixture (Sigma-Aldrich, St. Louis, Mo.) and then were plated in a 75-cm^2 flask (BD Biosciences, Bedford, Mass.) at a concentration of $10–15 \times 10^3$ cells/cm^2. Cells were cultured for 24 hours at 37° in an atmosphere of 5% CO_2 in air. Then the dishes were washed with PBS to remove nonadherent cells and cell fragments. The cells were maintained in culture in the same medium and under the same conditions until they reached approximately 80% confluence, with replacement of the culture medium every 3 to 4 days. Cells were then passaged with 0.05% trypsin-EDTA (Gibco, Invitrogen Corporation, Carlsbad, Calif.) at a dilution of 1:3. We used these cells (between passages 1 and 3) as ADSCs for transplantation, and characterization of ADSCs was performed using cells at passages 1 to 3. Furthermore, doubling time was determined by manually counting the number of cells.

In Vitro Differentiation of ADSCs

Adipogenic Differentiation

Adipogenic differentiation was performed by the method previously described by Lee et al[4] with slight modifications. To induce adipogenic differentiation, ADSCs were seeded at a density of 10^4 cells/cm^2 in 8-chamber slides (Nunc, Inc., Naperville, Ill.) and cultured in α-MEM (Nacalai Tesque, Kyoto, Japan) + 10% FBS until reaching 100% confluence; thereafter, the cells were further cultured for 21 days in the presence of 1 μM dexamethasone (Sigma-Aldrich, St. Louis, Mo.), 5 μg/mL recombinant human insulin (Wako Pure Chemical Industries, Ltd., Osaka, Japan), and 4.5 g/L glucose (Wako Pure Chemical Industries, Ltd., Osaka, Japan), as reagents for adipogenic differentiation. The cells cultured without these reagents (α-MEM + 10% FBS alone) served as a negative control. Adipogenic differentiation was confirmed by the formation of neutral lipid vacuoles stained with Oil Red O (Wako Pure Chemical Industries, Ltd., Osaka, Japan). For the Oil Red O stain, cells were fixed with 10% formalin, washed, and stained with a working solution of 0.18% Oil Red O for 5 minutes. The nuclei were counterstained with Mayer's hematoxylin solution (Wako Pure Chemical Industries, Ltd., Osaka, Japan).

Osteogenic Differentiation

To promote osteogenic differentiation, ADSCs were seeded at a density of 1×10^4 cells/cm^2 in 8-chamber slides and cultured in DMEM + 10% FBS until they reached 70% to 80% confluence. Osteogenic differentiation of ADSCs was induced by culturing them for 4 weeks with the osteogenic induction medium, which consisted of 0.1 μM dexamethasone (Sigma-Aldrich, St. Louis, Mo.), 10 mM β-glycerophosphate (Sigma-Aldrich, St. Louis, Mo.), and 0.2 mM ascorbate (Sigma-Aldrich, St. Louis, Mo.).[7] The cells cultured without these reagents (DMEM + 10% FBS alone) served as a negative control. Osteogenic differentiation was confirmed by the increased expression of alkaline phosphatase (ALP) by histochemical staining (TRACP & ALP double-stain kit; TAKARA BIO, Otsu, Shiga, Japan) and also by von Kossa

staining determining the deposition of the hydroxyapatite matrix.

Neural Differentiation

Neural differentiation of ADSCs was carried out according to the method described elsewhere (Woodbury et al, 2000).[8] Briefly, subconfluent ADSCs (70%–80% confluence) were cultured for 24 hours in preinduction medium [DMEM, 20% FBS, 1 mM β-mercaptoethanol (Wako Pure Chemical Industries, Ltd., Osaka, Japan)], and the cells were further incubated in the neurogenic medium (NM), which consisted of DMEM and 10 mM β-mercaptoethanol.[9] Neural differentiation was immunohistochemically determined by the expression of neural-specific enolase (NSE; BIOMOL International, Butler Pike Plymouth Meeting, Penn.).

Epithelial Differentiation

For epithelial differentiation, ADSCs were incubated with ATRA (Wako Pure Chemical Industries, Ltd., Osaka, Japan) at a final concentration of 5 μM as previously described by Brzoska et al.[10] The cells incubated without ATRA [the equivalent volume of DMSO (Nacalai Tesque, Kyoto, Japan), solvent for ATRA, was added to the culture] served as a negative control. The medium was replaced every 2 days during a total incubation period of 10 days. Differentiation was immunohistochemically and flow-cytometrically determined by the expression of cytokeratin-18 because of the preferential expression of the "primary" keratins on the intestinal epithelia.

Flowcytometry

Freshly isolated undifferentiated ADSCs (passages 0–3) were stained with unconjugated FITC- or PE-labeled monoclonal antibody (mAb) against CD11b, CD45, or CD90 (CALTAG Laboratories, Invitrogen Corporation, Carlsbad, Calif.), CD31 (Becto-Dickinson, Franklin Lakes, NJ), CD34 (Santa Cruz Biotechnology, Inc. Santa Cruz, Calif.). FITC-labeled goat antimouse IgG (BD Biosciences, San Jose, Calif.) was used as secondary antibody when necessary. In the case of staining with anti-cytokeratin-18 mAb, cells were fixed and permeabilized with Cytofix/Cytoperm solution (BD Biosciences, San Jose, Calif.). The cells thus treated were intracytoplasmically stained with FITC-anti-cytokeratin-18 Ab (PROGEN Biotechnik, Heidelberg, Germany). The stained cells were analyzed by a FACScan (BD Bioscience, San Jose, Calif.).

Measurement of HGF, VEGF, TGF-β, and Adiponectin

ADSCs were cultured in standard 12-well plates until 80% confluence and then culture supernatant was collected. The concentration of HGF (Institute of Immunology Co., Ltd., Tokyo, Japan), VEGF (R&D Systems, Minneapolis, MN), TGF-β (BioSource International, Inc., Camarillo, Calif.), and adiponectin (AdipoGen, Inc., Seoul, Korea) was measured by ELISA according to the manufacturers' instructions.

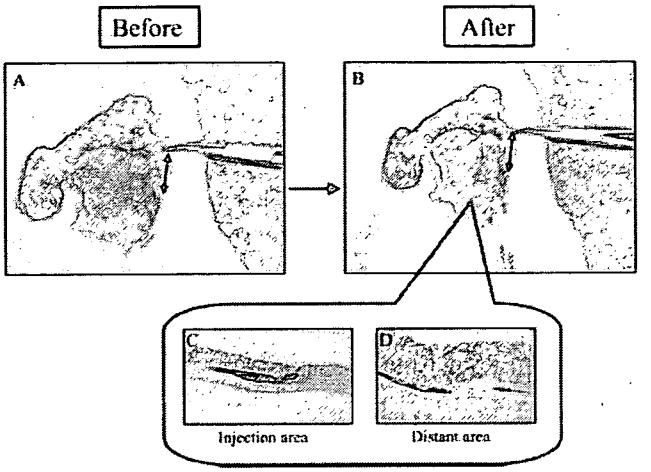

FIGURE 1. Procedure of submucosal injection. A: Under diethyl ether anesthesia, the intestine was exposed by a midline incision of the abdomen (blue arrow indicates the ulcer area injured by the TNBS injection) B: ADSCs or PBS (negative control) were injected from the serosa side into the submucosal layer. C: Using India ink, we confirmed that ADSCs were actually injected into the submucosal layer by this method. D: India ink was found in the submucosal layer of the area distant from the injection point.

In Vivo Examination

Induction of Colitis by TNBS

Colitis was induced by TNBS using the method described previously.[11] Briefly, rats were anesthetized after a 24-hour fast. Then an infant tube (indwelling feeding tube for infants, 4Fr, diameter = 1.35 mm; Atom Medical Co., Tokyo, Japan) was inserted into the anus, and the tip was advanced to 6 cm proximal in the colon. TNBS (Wako Pure Chemical Industries, Ltd., Osaka, Japan) dissolved in 50% ethanol was instilled into the colon through the cannula (30 mg of TNBS in a volume of 0.5 mL). After the instillation, the rats were held upside down by their tails for 60 seconds and then returned to their cages. We prepared more than 40 rats, and colitis was observed in all the rats injected with TNBS. Similarly, rats instilled with PBS served as controls (n = 10). All rats were sacrificed 10 days after administration of TNBS.

Submucosal Injection of ADSCs

ADSCs (passages 0–3), harvested from the culture by trypsin/EDTA solution, were suspended at 10^7 cells in 0.5 mL of PBS containing 2% FBS. Under diethyl ether anesthesia, the intestine was exposed by a midline incision of the abdomen, and ADSCs (10^7 cells) were injected from the serosa into the submucosa of the colon 2 days after the TNBS injection (n = 10; Fig. 1). Rats injected with 0.5 mL of PBS containing

2% FBS served as controls (n = 10).

Furthermore, using India ink, we confirmed that ADSCs were actually injected into the submucosal layer by this method, and India ink was found in the submucosal layer of 9 of the 10 rats injected with India ink (90%). It is noted that no complications were observed after the injection of 0.5 mL of ADSCs or PBS into the submucosa.

Assessment of Inflammation in TNBS-Induced Colitis

To examine the severity of colitis, the body weight of the treated rats was measured every other day, and clinical findings such as area of ulcer (measured using NIH image software on the pictures of colon), length (colocecal junction to anal verge), and weight of the colon 10 days after the TNBS injection were also assessed.

Histological Examination

The tissue specimens were fixed in buffered formalin and embedded in paraffin, and tissue sections were stained by H&E. Colonic inflammation was assessed using modification of the histopathologic grading system of Macpherson and Pfeiffer[12,13]: grade 0 = normal findings; grade 1 = mild mucosal and/or submucosal inflammatory infiltrate (admixture of neutrophils) and edema, punctate mucosal erosions often associated with capillary proliferation, muscularis mucosae intact; grade 2 = grade 1 changes involving 50% of the specimen; grade 3 = prominent inflammatory infiltrate and edema (neutrophils usually predominating), frequently with deeper areas of ulceration extending through the muscularis mucosae into the submucosa, rare inflammatory cells invading the muscularis propria but without muscle necrosis; grade 4 = grade 3 changes involving 50% of the specimen; grade 5 = extensive ulceration with coagulative necrosis bordered inferiorly by numerous neutrophils and lesser numbers of mononuclear cells, necrosis extends deeply into the muscularis propria; grade 6 = grade 5 changes involving 50% of the specimen. All scoring was performed by the same individual under blind conditions.

Measurement of Myeloperoxidase Activity

Tissue myeloperoxidase (MPO) activity was determined by a standard enzymatic procedure as previously described by Krawisz et al[14] with slight modifications. Total protein concentrations of the tissue supernatant and whole-cell lysate were measured using a BCA Protein Assay Kit (PIERCE Co., Rockford, Ill.) for calibration, and myeloperoxidase activity in the tissue homogenate was determined using a Myeloperoxidase Assay Kit (CytoStore Inc., Calgary, Alberta, Canada) according to the manufacturer's instructions.

Measurement of Cytokines in Colonic Tissue

The colonic tissue was homogenized in cold PBS using a Polytron-type homogenizer. Tissue homogenate was then centrifuged at 20,000g for 20 minutes at 4°C to obtain the supernatant. Total protein concentrations of the tissue supernatant and whole-cell lysate were measured using a BCA Protein Assay Kit (PIERCE Co., Rockford, Ill.) for calibration, and protein concentrations of IL-1β (BioSource International, Inc., Camarillo, Calif.), GRO/CINC-1 (functionally equivalent to IL-8; Panafarm Laboratory, Kumamoto, Japan), TNF-α (BioSource International, Inc., Camarillo, Calif.), and IFN-γ (BioSource International, Inc., Camarillo, Calif.) in the tissue homogenate were determined using ELISA kits according to the manufacturers' instructions.

In Situ Cell Proliferation

To evaluate proliferation of the colonic epithelium, 50 mg/kg of 5-bromo-2′-deoxyuridine (BrdU; Wako Pure Chemical Industries, Ltd., Osaka, Japan) was injected intraperitoneally 1 hour before sacrifice, and cells synthesizing DNA were immunohistochemically identified using a BrdU In-Situ Detection Kit (BD Biosciences, San Jose, Calif.) according to the manufacturer's instructions. We then counted the BrdU-positive cells in 10 crypts of the mucosa-bordering ulcer.

Y-Chromosome Fluorescence in Situ Hybridization (Y-FISH)

For assessment of distribution of ADSCs injected into the submucosa, in vivo experiments were performed in sex-mismatched conditions. TNBS-induced colitis models were prepared in female rats, and ADSCs obtained from male rats were injected into the submucosa of the colon in TNBS-induced colitis models. To detect the Y chromosome of ADSCs, we used a STAR-FISH Rat 12/Y Paint (Y FITC; 12 biotin) probe purchased from Cambio (Dry Drayton, Cambridge, UK), and detection protocols were conducted with a Histology FISH Accessory Kit (Dako Cytomation, Dako, Denmark).

Immunofluorescent Staining

Following Y-FISH, colonic tissues in paraffin-embedded sections (3 μm) were stained with mouse mAb against pan-cytokeratin (CHEMICON, now part of Millipore Corporation, Billerica, Mass.), vimentin (Santa Cruz Biotechnology, Inc. Santa Cruz, Calif.), S-100 (COSMO Bio Co., Ltd., Tokyo, Japan) or SMA (Lab Vision Corporation, Fremont, Calif.) after pretreatment procedure (epitope retrieval). They were then stained with PE-labeled goat antimouse IgG antibody (BD Biosciences, San Jose, Calif.). Cellular nuclei were counterstained with DAPI. Images were captured by a LSM510-META and exported as TIFF files and further processed in Adobe PhotoShop.

Statistical Analysis and Ethical Considerations

Results are expressed as mean ± SDs. Differences between groups were examined for statistical significance using the

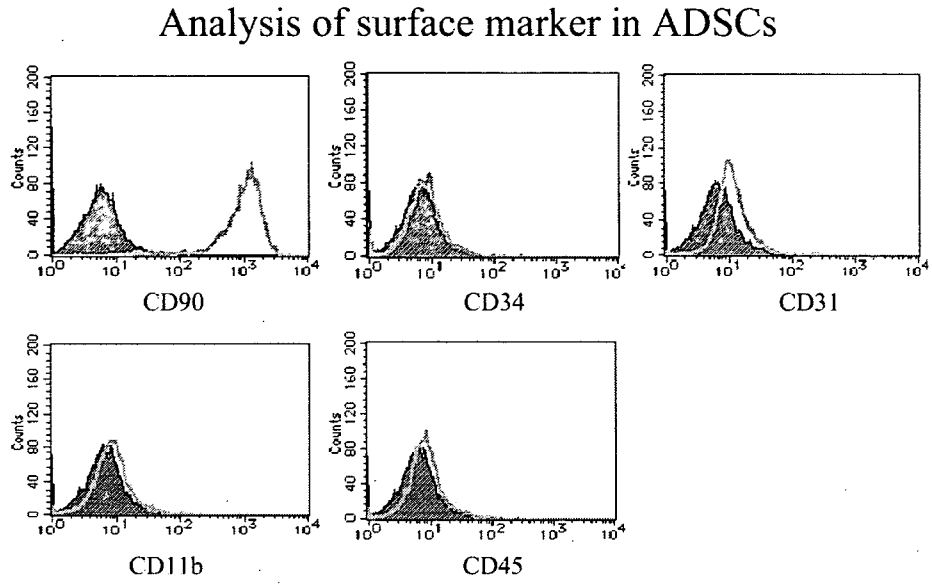

FIGURE 2. Characterization of ADSCs. ADSCs (passage 3) were flow-cytometrically characterized using antibodies against CD11b, CD31, CD34, CD45, and CD90. Cells stained with mAbs are represented by solid pink lines, and those stained with isotype-matched Ig, as negative controls, are represented by green lines. Cells were negative for CD11b, CD34, and CD45 but positive for CD90 and weakly positive for CD31.

Mann-Whitney test. The statistical analysis for the survival rate was performed by log rank test. A P value less than .05 was considered statistically significant. The experimental protocol was approved by the Ethics Review Committee for Animal Experimentation of Kansai Medical University.

RESULTS

Characterization of ADSCs from Subcutaneous Adipose Tissue

ADSCs were flow-cytometrically characterized (after 3 passages) and possible contaminants of hemopoietic lineage cells were excluded. ADSCs were negative for CD11b, CD34, and CD45 but positive for CD90 as shown in Figure 2, indicating that the ADSCs used in our experiments are not in the hemopoietic cell lineages. It is noted that a slight shift in the entire histogram was observed after staining with anti-CD31, indicating that ADSCs seem to be weakly positive for CD31. Furthermore, the doubling time of ADSCs remained unchanged (approximately 36–40 hours) up to 10 passages (Fig. 3). However, their growth stopped at 15 passages.

ADSCs Exhibit Multilineage Potential

We next examined the capacity of ADSCs to differentiate into multilineage cells under the appropriate culture conditions. ADSCs differentiated into adipocytes, osteocytes, neu-

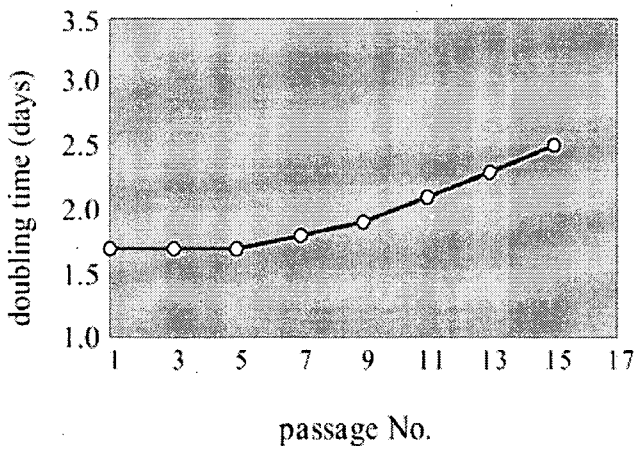

FIGURE 3. Doubling time of ADSCs. Doubling time (day) of ADSCs was determined at the indicated number of passages in DMEM.

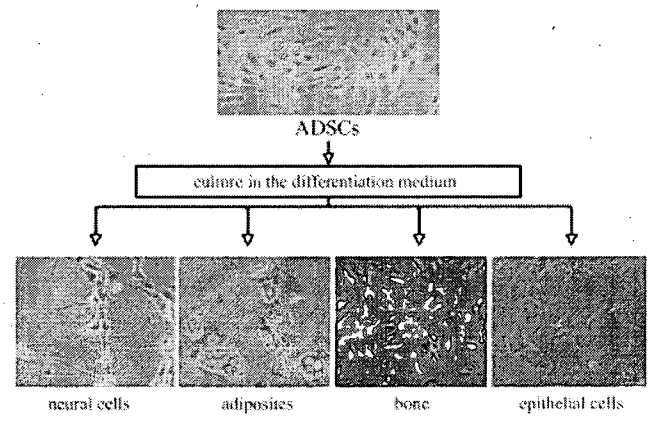

FIGURE 4. Culture of ADSCs. Multilineage differentiation was observed in the appropriate culture condition (bottom). Undifferentiated ADSCs showed multiple layers in the control culture medium.

rogenic cells, and epithelial cells using lineage-specific induction factors. Undifferentiated ADSCs cultured in the medium alone showed multiple layers. Neurogenic differentiation was confirmed by the expression of NSE in the cells with a neuronal morphology (Figs. 4 and 5), and adipogenesis was examined by Oil Red-O staining (Figs. 4 and 5). No lipid droplets stainable with Oil Red-O were observed in undifferentiated ADSCs. Differentiation toward osteocytes was determined by calcification of the extracellular matrix using von Kossa/alkaline phosphatase staining. ADSCs cultured in the epitheliogenic condition (5 μM ATRA for 10 days) showed a morphology resembling epithelial cells (Fig. 4), and they

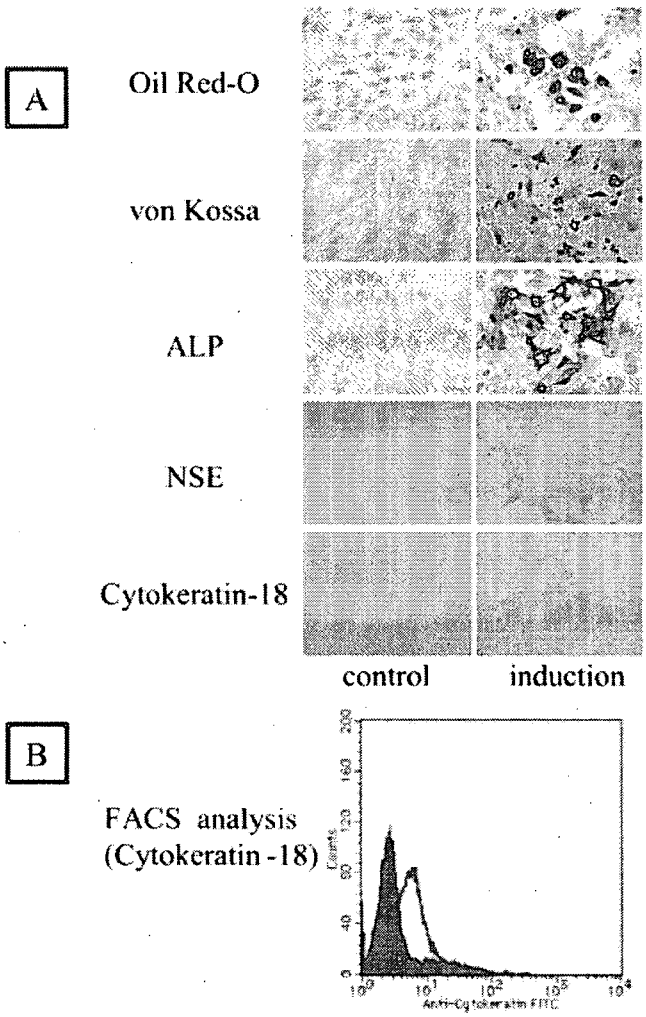

FIGURE 5. Immunohistochemical analyses of ADSCs after differentiation. ADSCs were cultured for 2–4 weeks in adipogenic, osteogenic, neurogenic, or epitheliogenic medium. A: ADSCs thus cultured were stained with Oil Red-O, von Kossa, alkaline phosphatase, NSE, or cytokeratin-18 to identify their differentiation. B: ADSCs cultured with epitheliogenic medium were flow-cytometrically analyzed after staining with FITC-anti-cytokeratin-18 mAb.

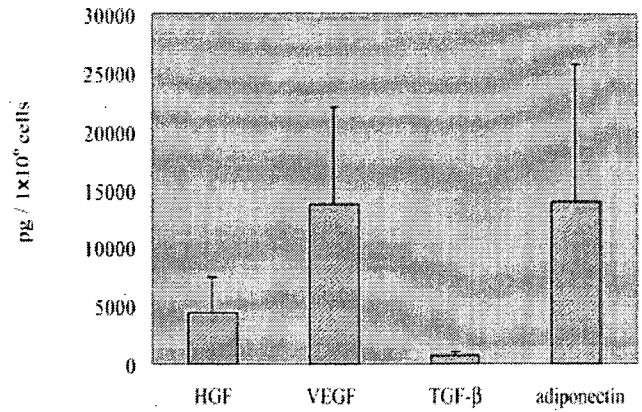

FIGURE 6. Secretion of HGF, VEGF, TGF-β and adiponectin by ADSCs. ADSCs were cultured for 1 week, and the amounts of HGF, VEGF, TGF-β, and adiponectin were measured by ELISA. Columns and bars represent the means ± SDs of 14 samples.

were positive for cytokeratin 18 as shown in Figure 5, where a filamentous cytoskeleton, the typical appearance of epithelial cytokeratins, was stained with this mAb. This was flow-cytometrically confirmed after staining with FITC-anti-cytokeratin-18 mAb (Fig. 5B).

ADSCs Secrete VEGF, HGF, TGF-β, and Adiponectin

The secretion of HGF, VEGF, TGF-β , and adiponectin from ADSCs was examined. They secreted significant amounts of VEGF (13,654 ± 3185 pg/10^6 cells), HGF (4434 ± 1140 pg/10^6 cells), and adiponectin (13,910 ± 5902 pg/10^6 cells) but only minimal amounts (733 ± 136 pg/10^6 cells) of TGF-β (Fig. 6).

Inoculation of ADSCs Reduces Severity of TNBS-Induced Colitis

Changes in body weight, colon weight, and survival rate were evaluated for assessment of the severity of colitis (Fig. 7). There was no statistical significance in the changes in body weight or survival rate between the recipients of ADSCs and the recipients of PBS in TNBS-induced colitis-model rats. However, a significant decrease in colonic weight was observed in the recipients submucosally injected with ADSCs, suggesting that the colonic edema associated with inflammatory responses was ameliorated by the inoculation of ADSCs. Although the results shown in Figure 7 represent only 2 replicate experiments, the values and outcomes in the other experiment were similar to those in Figure 7.

Inoculation of ADSCs Facilitates Repair of Colonic Ulcers

Next, we examined the effects of ADSCs on the repair of colonic ulcers. Eight days after the submucosal injection of ADSCs (or PBS), rats were sacrificed, and the area of colonic

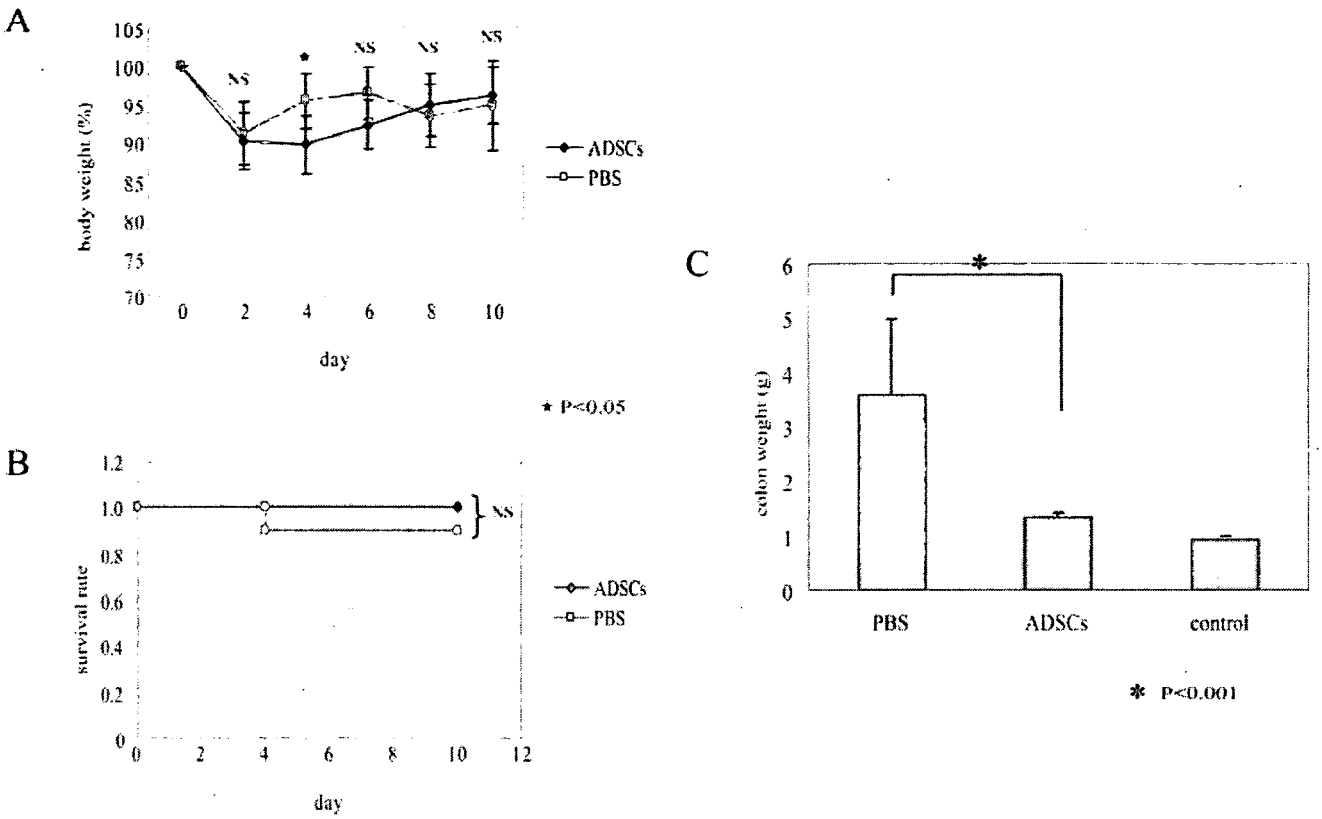

FIGURE 7. Measurement of body and colonic weight and survival rate after inoculating the colitis-model rats with ADSCs. A: Body weight was measured every 2 days, and colonic weight was determined 8 days after the injection of ADSCs (10 days after the injection of TNBS). It is noted that there was no statistically significance difference in body weight between the recipients of PBS and the recipients of ADSCs (except on day 4). B: Effects of ADSCs on survival rate were examined. Statistical analysis was performed by the log rank test. C: Colonic weight was measured 8 days after the submucosal injection of ADSCs. The results are representative of 2 replicate experiments. Symbols, columns, and bars represent the means ± SDs of 10 rats ($^*P < 0.001$).

ulcers and colon length were measured (Fig. 8A). As shown in Figure 8B, the ulcer area was significantly reduced (23 ± 2 mm^2) in the TBNS-induced-colitis rats treated with ADSCs compared with those treated with PBS (65 ± 13 mm^2; $P < 0.05$). However, there was no statistically significant difference in colonic length between the rats treated with ADSCs (15.2 ± 0.2 cm) and the rats treated with PBS (15.3 ± 0.8 cm; Fig. 8C). Furthermore, we evaluated the proliferation of colonic epithelium (photographed in Fig. 8D,E) by the injection of BrdU. When the colitis-induced rats were treated with ADSCs, the number of BrdU-positive cells significantly increased in the mucosal epithelium surrounding colonic ulcers when compared with those treated with PBS (treated with ADSCs, 28.1 ± 3.6/crypt, versus treated with PBS, 18.9 ± 4.0/crypt; $P < 0.05$; Fig. 8F).

Inoculation of ADSCs Ameliorates Colitis

Histological examination was carried out to determine whether ADSCs could reduce the inflammation induced by TNBS. Extensive ulceration with coagulative necrosis extending into the muscularis propria was observed in the untreated (PBS-injected) group, and numerous neutrophils (and relatively small numbers of mononuclear cells) were detected as inflammatory cells (Fig. 9A). In contrast with these findings, in the group injected with ADSCs, a decrease in the infiltration of inflammatory cells was clearly observed along with amelioration of edema and the concomitant enhancement of epithelial regeneration, as shown in Figure 9B. Histological score is summarized in Figure 9C.

MPO activity, an index of inflammatory response, was next determined in the colon in order to evaluate the degree of inflammation in the rats treated with ADSCs or PBS after the induction of colitis by TNBS. A significant increase in MPO activity was observed in the injured colon of colitis-model rats, and the injection of ADSCs (but not PBS) was able to reduce the local MPO activity (Fig. 9D). In addition, other inflammatory cytokines, such as TNF-α, IFN-γ, IL-1β,

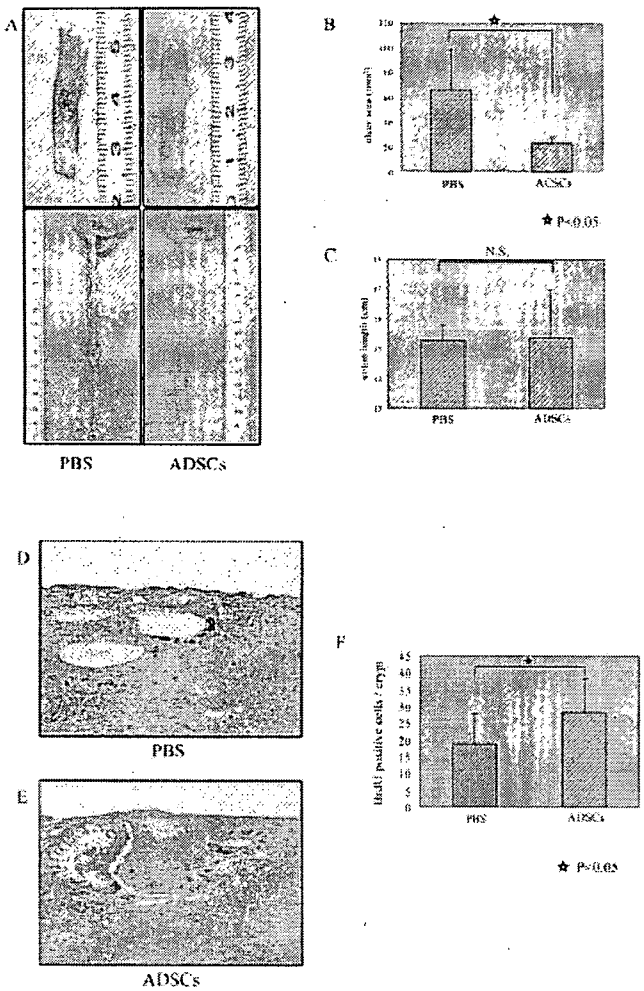

FIGURE 8. Effects of ADSCs in the repair of colonic ulcer. ADSCs or PBS submucosally injected into colitis-induced rats. A: Macroscopic examination of the area of colonic ulcers and the colon 8 days after the submucosal injection of ADSCs or PBS. B: Area of the ulcer was measured using NIH image software on pictures of the colon. C: Length (colocecal junction to anal verge) of the colon was measured by a scale. D, E: Proliferation of colonic epithelial cells was measured by injection of BrdU into rats treated with ADSCs or PBS. Representative photographs of PBS and ADSCs are shown in D and E, respectively (magnification ×400). F: BrdU-positive cells were counted, and the number of positive cells per crypt was calculated. Columns and bars represent the means ± SDs of 10 rats.

and IL-8, were examined. The expression of GRO/CINC-1 (functionally equivalent to IL-8), but not of IL-1β, TNF-α, or IFN-γ was reduced by the injection of ADSCs into the colitis-model rats (data not shown). These findings clearly show that ADSCs can ameliorate an inflammatory reaction and reduce the level of some inflammatory cytokines induced by the injection of TNBS.

Distribution and Differentiation of ADSCs In Vivo

We carried out ex vivo studies to determine whether ADSCs can differentiate into the colonic mucosa. We examined the presence of ADSCs (or ADSC-derived cells) submucosally injected by tracing Y-chromosome-positive cells with FISH (Fig. 10A–E). When compared with normal uninjured mucosal area, more than 3 times the number of ADSCs were detected in the ulcer area (22.2 ± 4.7 versus 54.4 ± 17.4 cells/field, $P < 0.05$; Fig. 10F). Most of the ADSCs were observed in the submucosal layer, whereas some were observed in the mucosal layer and in the muscularis propria. No Y-chromosome-positive cells (ADSC-derived cells) were observed in the epithelial cells, vessel component, or nerve cells (data not shown). Furthermore, Y-chromosome-positive cells were determined after staining with cytokeratin, vimentin, S-100, or SMA in order to characterize cells of ADSC origin (Fig. 11). Y-chromosome-positive cells were detected in fibroblast-like cells under the basal membrane, in smooth muscle cells in the muscle layer, and in adipose tissue. However, they were not detected in endothelial cells, the neural crest, and epithelial cells.

DISCUSSION

In the present study, we have shown that ADSCs can facilitate colonic mucosal repair and reduce the infiltration of inflammatory cells. The ADSCs used in the present study were characterized as $CD90^{+}CD45^{-}$ cells,[15,16] being similar to bone marrow–derived mesenchymal stem cells (MSCs),[1,3,4,7] and they were cytohistochemically confirmed to be functional MSCs (Figs. 4 and 5) because of their capacity to differentiate into cells with adipogenic, osteogenic, neurogenic, and epitheliogenic lineages when lineage-specific induction factors have been added to the culture, as has been previously reported.[2,9,17,18] Therefore, the ADSCs used in the present study have similar features to MSCs from the bone marrow. The proliferative capacity of the ADSCs was also similar to that of MSCs.[4,7,15,16] The doubling time of ADSCs remained unchanged until 10 passages (Fig. 3). Therefore, along with the ADSCs being easily obtained by lipoaspiration,[19] ADSCs can be a useful candidate for the source of cell therapy.

In addition, one advantage of ADSCs is their potential to secrete growth factors, such as VEGF, HGF,[20] and adiponectin,[21] which facilitate the regeneration of injured tissue alone or synergistically.[22] As has been reported, HGF regulates cell growth, motility, and morphogenesis of various types of cells, including epithelial cells and endothelial cells, and it also prevents fibrosis.[23,24] Recent studies have shown that the combination of HGF with VEGF increases neovascularization in the rat corneal assay[25] and that HGF facilitates the repair of large colonic ulcers in TNBS-induced colitis in rats.[26] Adiponectin has been reported to not only improve insulin resistance and prevent atherosclerosis, fatty liver, and

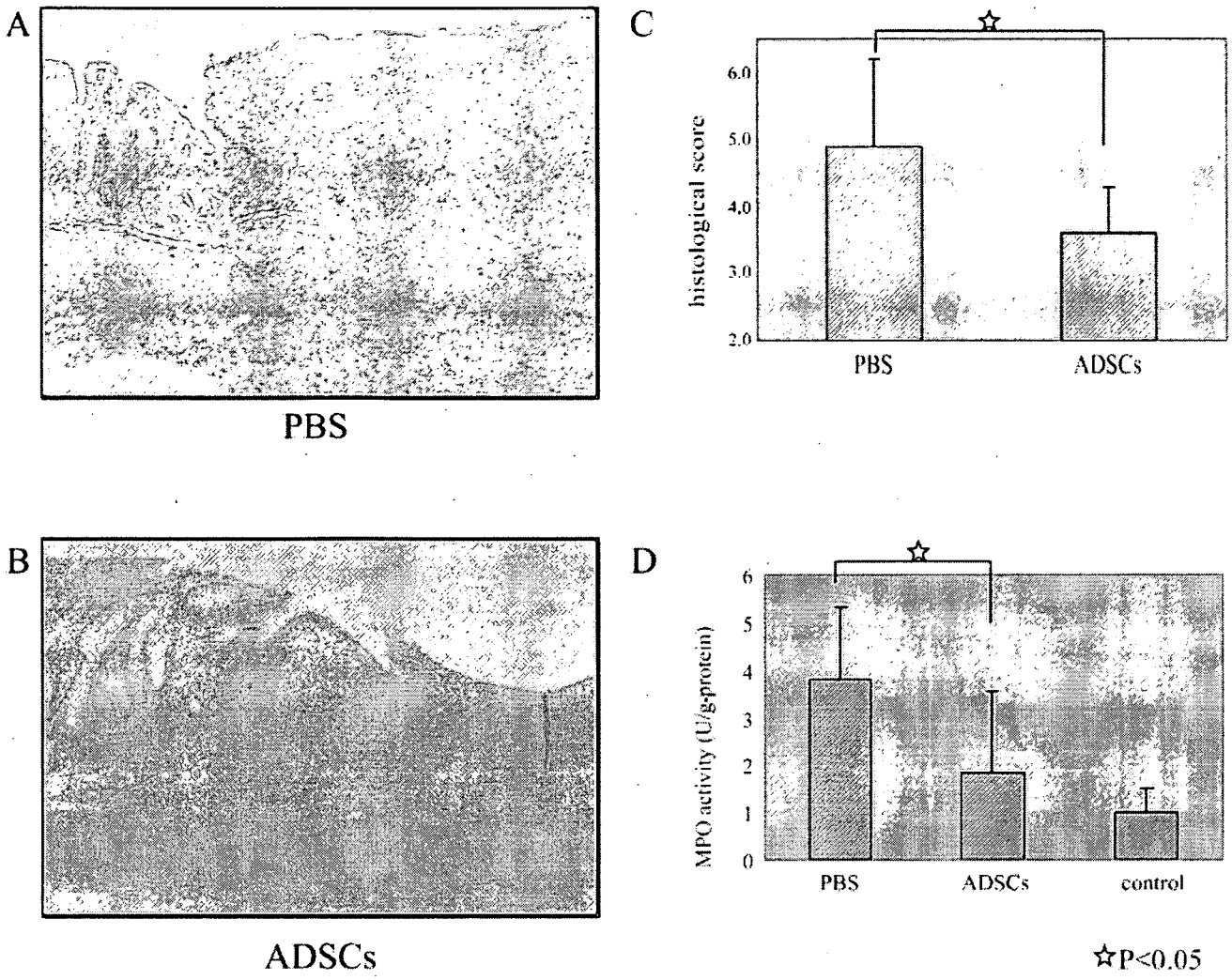

FIGURE 9. Amelioration of colitis and reduction of inflammatory responses by ADSCs. A: Histopathologic examination of colon was carried out in TNBS-induced colitis rats injected with PBS. It is noted that extensive mucosal damage and marked inflammatory cell infiltration were observed. B: Histopathologic examination of colon 8 days after injection of ADSCs; the development of regenerative epithelium, and reduced inflammatory cell infiltration and edema were observed (magnification ×100). C: Histological score of rats injected with PBS or ADSCs. D: Measurement of MPO activity. Colonic MPO activity determined 10 days after injection of PBS or ADSCs in colitis-induced rats. The rats injected with PBS alone (without injection of TNBS or ADSCs) served as controls. Columns and bars represent the means ± SDs of 10 rats ($^*P < 0.05$).

liver fibrosis but also to exert several anti-inflammatory effects.[27–30] Moreover, it has been reported that adiponectin reduces the attachment of monocytes to the endothelium by down-regulating the expression of vascular cell adhesion molecule–1, intercellular adhesion molecule-1, and E-selectin[27] and that it inhibits phagocytic activity and production of TNF-α and IL-6 from cultured macrophages.[31] These results indicate that HGF, VEGF, and adiponectin play a crucial role in intestinal mucosal wound healing. In the present study, significant amounts of HGF, VEGF, and adiponectin were detected in the culture supernatants of ADSCs (Fig. 6), indicating that ADSCs injected into the submucosa may secrete these cytokines in situ, resulting in the acceleration of regeneration of wound mucosa and also inhibition of the inflammation observed in TNBS-induced colitis. This possibility was actually confirmed by the in vivo examination in which ADSCs facilitated the repair of colonic ulcers (Fig. 8) and reduced inflammatory responses along with TNBS-induced colitis (Fig. 9). There was no statistically significant differences in colon length between the group submucosally injected with ADSCs and the group injected with PBS. This might have been a result of the large ulcer being detected in a limited area of colon in TNBS-induced colitis-model rats in contrast to pan-colitis-model rats.

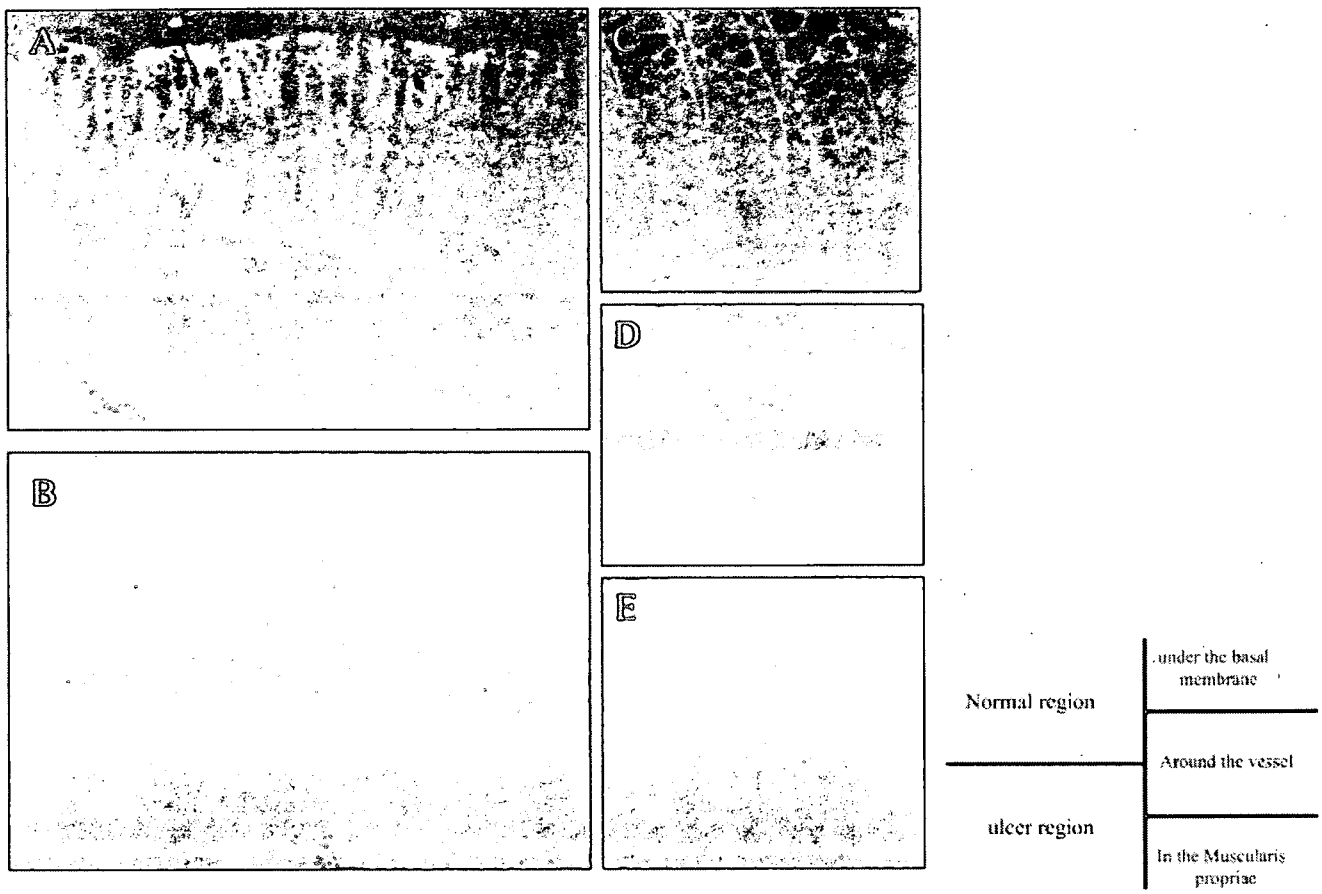
A
B
C
D
E
Normal region
ulcer region
under the basal membrane
Around the vessel
In the Muscularis propriae

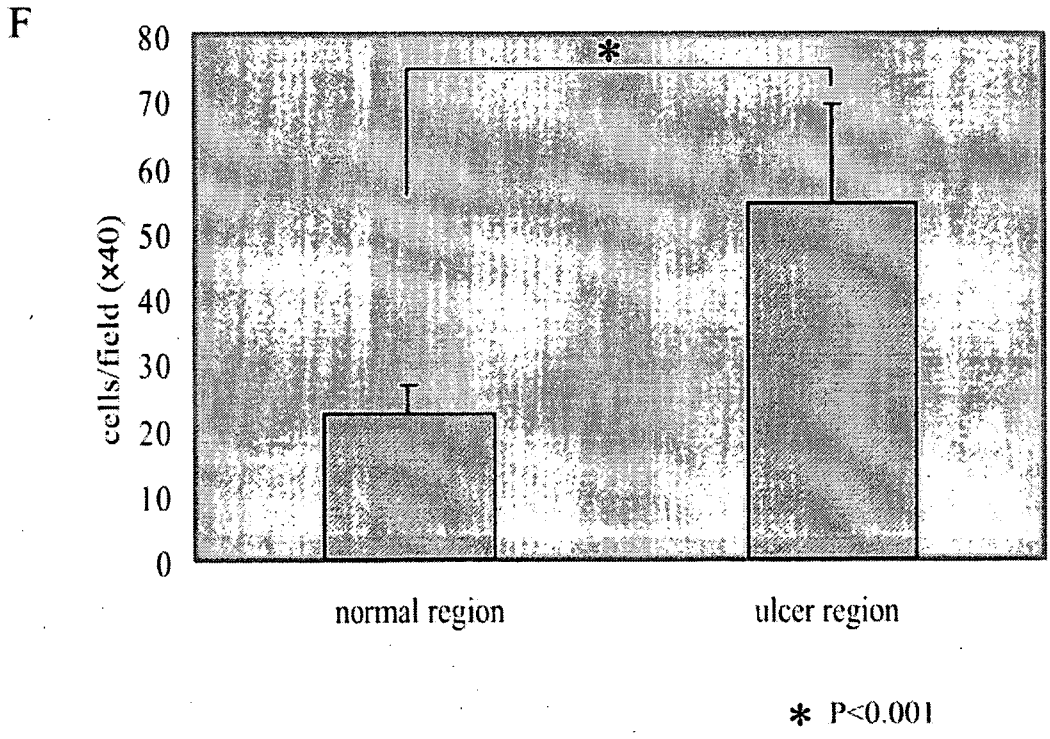
F
cells/field (x40)
80
70
60
50
40
30
20
10
0
*
normal region
ulcer region
* P<0.001

10